Supplemental Material for:

Mutation-independent Rhodopsin Gene Therapy by Knockdown and Replacement with a Single AAV vector

Artur V. Cideciyan[a,1], Raghavi Sudharsan[b], Valérie L. Dufour[b], Michael T. Massengill[c], Simone Iwabe[b], Malgorzata Swider[a], Brianna Lisi[a], Alexander Sumaroka[a], Luis Felipe Marinho[b], Tatyana Appelbaum[b], Brian Rossmiller[c], William W. Hauswirth[d], Samuel G. Jacobson[a], Alfred S. Lewin[c,2], Gustavo D. Aguirre[b], William A. Beltran[b,1,2]

[a]Scheie Eye Institute, Department of Ophthalmology, University of Pennsylvania Perelman School of Medicine, Philadelphia, Pennsylvania 19104 USA; [b]Division of Experimental Retinal Therapies, Department of Clinical Sciences & Advanced Medicine, School of Veterinary Medicine, University of Pennsylvania, Philadelphia, Pennsylvania 19104 USA; [c]Department of Molecular Genetics & Microbiology, University of Florida, Gainesville, Florida 32610; [d]Department of Ophthalmology, University of Florida, Gainesville, Florida 32610.

[1]These authors contributed equally to this work.

[2]To whom correspondence should be addressed.

E-mails: wbeltran@vet.upenn.edu, lewin@ufl.edu

www.pnas.org/cgi/doi/10.1073/pnas.1805055115

SUPPLEMENTAL RESULTS

Suppression of canine RHO with *Rz525*

A hammerhead ribozyme (*Rz525*) that was shown in an *in vitro* assay (Suppl. Fig. S2) to reduce the expression of WT human RHO, was packaged in an AAV2/5 vector and subretinally injected in three WT canine eyes at 20 and 50x10^{11} vg/mL titers (Suppl. Fig. S3A). The efficiency of AAV2/5-*Rz525* at reducing expression of endogenous canine RHO at the RNA level was measured only in the eye injected with the highest titer (50x10^{11} vg/mL). In the treated area there was complete silencing of RHO expression at the RNA level (Suppl. Fig. S3B) while RHO protein levels were reduced to ~30% (Suppl. Fig. S3C). The two eyes injected with a 20x10^{11} vg/ml had higher (47 and 64%) levels of endogenous canine RHO protein remaining in the treated areas (Suppl. Fig. S3C).

Rz525 was subsequently tested in five heterozygous *RHO*-mutant eyes (Suppl. Table S1 grp F) that were subretinally-injected with AAV2/5-*Rz525* at either 20x10^{11} (3 eyes) or 100x10^{11} vg/mL (2 eyes). An additional mutant eye was injected with BSS and served as a negative control. At 8 weeks post injection, prominent silencing of RHO expression was seen with the highest titer (100x10^{11} vg/mL) both at RNA (13% remaining) and protein (0.1% remaining) levels in the treated area of EM396-OD (Suppl. Fig. S4A-C). However, this treatment was associated with signs of retinal detachment and cellular infiltration in the subretinal space detected by OCT imaging (Suppl. Fig. S4E, upper row), and confirmed by histology in the fellow eye (EM396-OS) injected with a similar titer (Suppl. Fig. S4E, lower row). Two eyes injected with the lower

20x10^{11}vg/mL titer had more endogenous canine RHO remaining within the treated area both at the RNA (39 and 66%) and protein (36 and 67%) levels (Suppl. Fig. S4A-C). To evaluate whether these levels of RHO suppression were sufficient to confer protection from light-induced retinal degeneration, two mutant-RHO eyes injected with AAV2/5-*Rz525* at 20 and 100x10^{11} vg/mL were exposed to light at 6 weeks post-injection and imaged by OCT. Two weeks after the light exposure, the eye injected with a titer of 100x10^{11} vg/mL had some regions of ONL retention within the treated area; however, no such rescue was seen in the eye injected with the lower (20x 10^{11} vg/mL) titer (Suppl. Fig. S4D).

These results showed that near complete knockdown of RHO could be achieved with *Rz525*, and that reduction of RHO protein expression was associated with some degree of protection against light-induced retinal degeneration in the canine model of *RHO*-adRP. Yet, protection could be achieved only when injecting high viral loads that were associated with severe signs of retinitis/chorioretinitis.

Limited suppression of WT canine RHO with *shRNA$_{131}$*

A knockdown reagent (*shRNA$_{131}$*) that had been shown to reduce expression of WT human RHO in cell culture (Fig. 1) was packaged in an AAV2/5 vector and subretinally injected in two WT canine eyes at 10 and 50x10^{11} vg/mL titers (Suppl. Fig. S5A; Suppl. Table S1 grp B). The efficiency of AAV2/5-*shRNA$_{131}$* at reducing expression of endogenous canine RHO both at the RNA and protein level was limited. Even with the highest titer (50x10^{11} vg/mL) there was still 50% of normal levels of endogenous canine *RHO* RNA (Suppl. Fig. S5B) and 70% of endogenous canine RHO

protein (Suppl. Fig. S5C) remaining within the treated areas 8 weeks post-injection. As a result, further investigations in dogs on the use of *shRNA*$_{131}$ as a potential candidate for RHO suppression were not pursued.

SUPPLEMENTAL METHODS

Ribozyme cleavage assay

HEK293T cells (CRL-11268, ATCC, Manassa, VA) were transfected with the dual luciferase plasmid psiCHECK™-2 (Promega, Madison, Wi) expressing a 100 nucleotide target region of either wild type or resistant (hardened) human *RHO* cDNA linked to the Renilla luciferase expressed by the SV40 promoter. *RHO* transcript levels were measured in six replicates by luciferase assay. The luciferase plasmid was co-transfected with a plasmid expressing *Rz525* from the tRNAval promoter. Results were normalized to the same fusion transcript measured following co-transfection with a plasmid lacking ribozyme.

Generation of the *RHO*-tGFP and *RHO*$_{820}$-tGFP expressing plasmids

A plasmid containing the CMV-promoter, the human WT-*RHO* open reading frame (ORF) with a C-terminal turboGFP tag, and BGH-PolyA signal (also encoding ampicillin resistance and neomycin resistance genes) was used to express *RHO in vitro*. P23H *RHO,* T17M *RHO,* and *RHO*$_{820}$ versions of the CMV-hRHO-turboGFP-BGH-PolyA plasmid were created using the Q5® Site-Directed Mutagenesis Kit (New England Biosciences, Ipswich, MA., USA) according to the manufacturer's instructions, except with

the PCR parameters described here. To generate the P23H RHO version, the 23rd codon of the hRHO ORF of the CMV-hRHO-turboGFP-BGH-PolyA plasmid was changed from CCC to CAC with the following primers: Forward – CACACCCGTCGCATTGGA, and Reverse - GTACGCAGCCACTTCGAGTAC. To produce the *RHO*$_{820}$ version, nucleotides 816 to 825 of the hRHO ORF in the CMV-hRHO-turboGFP-BGH-PolyA plasmid were changed from ATTCTACATC to TTTTTATATA with the following primers: Forward: ATATATTCACCCACCAGGGCTCCAAC, and Reverse: AAAAAGCCA CGCTGGCGTAGGGC. The PCR reaction parameters were as follows: initial denaturation at 98ºC for 30s, 25 cycles of denaturation (98ºC for 10 s, annealing for 30s, extension at 72ºC for 5 minutes), final extension at 72ºC for 2 minutes. The annealing temperatures used for the P23H *RHO* and *RHO*$_{820}$ PCR reactions were 68º and 72ºC, respectively. 25µg of the CMV-hRHO-turboGFP-BGH-PolyA plasmid was used as the template for each reaction. The AAV-T17M-GFP was a gift of Dr. Marina Gorbatyuk.(76)

In vitro screening of shRNA-mediated knockdown of RHO

HEK293T cells (ATCC) were seeded in a 12-well plate and transfected the following day when the cells reached 70-90% confluence. Into each well, 500 ng of the CMV-hRHO-turboGFP-BGH-PolyA plasmid expressing either wild-type human *RHO*, human P23H *RHO*, human T17M *RHO*, or *RHO*$_{820}$ (a human *RHO* made resistant to *shRNA*$_{820}$ degradation via four silent codon modifications) was transiently co-transfected with 1µg of a self-complementary rAAV2 plasmid containing an anti-sense GFP stuffer sequence and either a control H1-shRNA cassette, an on-target (131, 134, or 820) H1-shRNA cassette, or no (empty) H1-shRNA cassette. Each co-transfection condition was

performed in triplicate. A DNA to polyethylenimine (PEI at 1mg/mL; Polysciences Inc, Warrington, PA., USA) ratio of 1µg: 3µL was utilized such that each well received 4.5µL of PEI. The cells were incubated for 48 hours at 37ºC with 5% CO_2. Following incubation, the medium was aspirated, and the cells were re-suspended in phosphate buffered saline (PBS) and pelleted by centrifugation at 3,000xg. The PBS was then removed and the cells were re-suspended and sonicated in 150µL of 0.23M sucrose in PBS. 50µL of loading buffer (200 mM Tris-Cl pH 6.8 + 400 mM DTT + 8% SDS + 40% glycerol + bromophenol blue) was applied to each sample and mixed by pipetting. The samples were incubated at room temperature for 30 minutes before being passed through a 28-gauge insulin syringe to shear co-extracted DNA. The total protein concentration of each sample was measured using the Pierce™ 660nm Protein Assay Reagent and the Pierce Ionic Detergent Compatibility Reagent (Thermo Fisher, Waltham, MA., USA). The amount of total protein loaded in to each well (15-20 µg) was constant within each experiment. The samples were run on a 10% Mini-PROTEAN® TGX™ Precast Protein Gels (Biorad, Hercules, CA., USA) adjacent to the Li-COR Chameleon ladder (Li-Cor, Lincoln, NE, USA) and transferred to a iBlot PVDF Transfer Stack using Invitrogen's iBlot system (Invitrogen, Carlsbad, CA, USA) according to the manufacturer's instructions. Membranes were incubated with methanol for 5 minutes, washed with diH_2O 3 times, and blocked for 1 hour at room temperature with Odyssey blocking buffer (Li-Cor, Lincoln, NE, USA). Membranes were then incubated with mouse anti-TurboGFP (1:2000; Origene, Rockville, MD, USA) and rabbit anti-β-tubulin (1:5000; Millipore, Burlington, MA, USA) in blocking buffer overnight at 4ºC, and washed three times with 0.1% Tween20 in PBS before incubation with IRDye 800CW donkey-anti-rabbit and IRDye 680RD goat-anti-

mouse (Both 1:5,000; Li-Cor, Lincoln, NE, USA) for 45 minutes at room temperature. Membranes were washed three times with 0.1% Tween20 in PBS and imaged with an Odyssey CLx system (Li-Cor, Lincoln, NE, USA). Band intensity was measured with the ImageJ software. To measure the band intensity of the predicted monomeric form of RHO-GFP, a box was drawn around the prominent band appearing at ~65kDa whereas the aggregated forms were measured using a box drawn from the highest molecular weight marker (260kDa) to the visible band just below 50kDa. Band intensity of RHO was corrected for loading by measuring and dividing by the band intensity of β-tubulin. Values were reported as relative intensity, which was calculated as the corrected band intensity of each sample divided by the average corrected band intensity for the control shRNA condition. Statistical significance was determined via one-way ANOVA followed by Tukey's multiple comparisons test.

AAV vector preparation.

Adeno-associated virus (AAV) vectors with type 2 terminal repeats (TRs) were packaged in serotype 5 capsids as described by Zolotukhin *et al.* (2002).(79) Production of AAV-*shRNA*$_{820}$-*RHO*$_{820}$ started with the cotransfection of human embryonic kidney (HEK) 293T cells with two plasmids, the transgene plasmid sc-HOP-*RHO*$_{820}$-H1-*shRNA*$_{820}$ and the helper plasmid pXYZ5. AAV5 capsids permit efficient transduction of photoreceptor cells following subretinal injection.(78)

Vectors designed to knockdown human and canine rhodopsin without replacement, contained a 488 bp region (positions 916-1396) of the mouse *Rho* gene (GenBank

M55171.2) and a humanized GFP gene cloned in reverse orientation. This orientation was used to provide a spacer for efficient packaging of AAV without over-expression of GFP. For *RHO* expression in the RNA replacement vectors, a 536 bp region (positions 4547-5083) from the human *RHO* gene (GenBank Accession number NG_009115.1) was employed as the human rhodopsin proximal promoter (hOP). The promoter was followed by a 163 bp synthetic intron (SD/SA) from SV40 which preceded 125 bp from the *RHO* 5' UTR the human *RHO* cDNA (1046 bp), or a codon-modified version (*RHO_{820}*) made resistant to *$shRNA_{820}$* (see below). This was followed by a polyadenylation signal from SV40.

Name	Target sequence	Resistant Sequence
$shRNA_{131}$	CUGCCUACAUGUUUCUGCU	N/A
$shRNA_{134}$	CCUACAUGUUUCUGCUGAU	N/A
$shRNA_{820}$	GUGGCAUUCUACAUCUUCA	GUGGCUUUUUAUAUAUUCA
Rz525	GGUGGUCCUGGC	N/A

AAV2/5 vectors for shRNA expression were packaged as self-complementary AAV,(77) and expression of shRNAs was directed by the human H1 RNA promoter (GenBank X16612.1; nucleotides 276-378). The shRNAs contained 19 bp of double stranded sequence connected by a 9 nucleotide loop (TTCAAGAGA). For vectors intended for shRNA delivery without rhodopsin replacement, efficient packaging required maintenance of at least 2.2 kb of DNA between the terminal repeat sequences of AAV. In these vectors, the sequence of humanized GFP (80) was inserted in reverse orientation behind either the mouse opsin proximal promoter or the human opsin

proximal promoter (see above). The vector used to express hammerhead ribozyme Rz525, pMOPS500NewHpRz525, used the mouse proximal rhodopsin promoter to drive expression of the ribozyme cassette. It is was described by Gorbatyuk et al. 2007.(33)

Both *shRNA*$_{820}$ and a human rhodopsin cDNA (*RHO*$_{820}$) made resistant to *shRNA*$_{820}$ by introducing silent mutations in the target sequence were packaged together as self-complementary AAV2/5. A self-complementary construct was chosen to accelerate the rate of RHO replacement (with *RHO*$_{820}$) in order to preserve, or rapidly reform rod outer segment structure in the context of a highly efficient KD reagent (*shRNA*$_{820}$).

Animals

All dogs were bred and maintained at the University of Pennsylvania Retinal Disease Studies Facility (RDSF). Studies were carried out in strict accordance with the recommendations in the Guide for the Care and Use of Laboratory Animals of the National Institutes of Health and the USDA's Animal Welfare Act and Animal Welfare Regulations, and complied with the ARVO Statement for the Use of Animals in Ophthalmic and Vision Research. The protocols were approved by the Institutional Animal Care and Use Committee of the University of Pennsylvania.

All normal (WT dogs) were house under standard kennel cyclic (12 hrs ON, 12 hrs OFF) white light illumination (175-350 lux at the level of the "standard" dog eye). All *RHO*-mutant dogs studied were heterozygous for the T4R mutant allele, and are referred to in text as *RHO*-mutants, and as RHO$^{T4R/+}$ in Table S1 and in figures to emphasize the

heterozygosity. All but 3 mutant RHO dogs were housed under cyclic dim red illumination (9-20 lux at the level of the “standard” dog eye) from birth until termination to prevent any acceleration of retinal degeneration triggered by environmental white light. All electroretinographic and noninvasive imaging procedures, as well as subretinal injections, were performed under general anesthesia, as previously described.(44, 74, 81) Ocular tissues were collected after euthanasia with i.v. injection of euthanasia solution (Euthasol; Virbac), and all efforts were made to improve animal welfare and minimize discomfort. Included were 21 eyes from 14 normal (WT) dogs, and 40 eyes from 21 *RHO*-mutant dogs (Suppl. Table S1).

Subretinal injections

Subretinal injections of BSS or vector were performed under direct visualization through an operating microscope (Zeiss OPMI 6; Carl Zeiss Inc, Oberkochen, Germany) and a contact vitrectomy lens using a subretinal cannula as previously reported (65). In the case of the *RHO*-mutant dogs, dim red illumination was set up in the operating room, and subretinal injections were performed under near infrared light illumination using an infrared bandpass filter (RT-830; Hoya Optics, Inc, Fremont, California) placed in the operating miscroscope’s light path and monocular infrared image intensifiers (Owl Nitemare Third generation: BE Meyers & Co, Inc, Redmond, Washington) that were mounted on the two microscope eyepieces as previously described.(49) This night vision system allows the surgeon to perform subretinal injections in the light-sensitive *RHO*-mutant dogs without causing any surgical light-induced retinal degeneration.(49) Successful subretinal injection of a ~150 μL volume produced a bleb that covered ~15%

of the retinal surface. The location of the subretinal bleb was recorded immediately after each injection. This was done in normal dogs by fundus photography (Retcam shuttle, Clarity Medical Systems, Pleasanton, CA), and in *RHO*-mutant dogs by drawings of the bleb on near infrared cSLO composite images captured prior to the injection.

Experimental acceleration of retinal disease by a light exposure.

An acute light exposure protocol was used as previously described (46-48) to assess the efficiency of the viral vector constructs at preventing retinal degeneration in the light sensitive *RHO*-mutant dog.(45) All steps of this procedure were carried out under dim red light illumination. The pupils were dilated with 1% tropicamide and 1% phenylephrine (3 times, 30 min apart in both eyes), and general anesthesia was induced with propofol (4mg/kg) IV and maintained with inhalation anesthesia (isoflurane). To prevent the ventral rotation of the globe induced by the general anesthesia, a retrobulbar saline injection (5-10 ml) was performed to recenter the eyes in the primary gaze position. A one min exposure to white (6500K) light at a corneal irradiance of 1 mW/cm^2 (measured with a luminometer, IL1700; International Light Technologies, Peabody, MA, USA) was performed using a monocular Ganzfeld stimulator (ColorBurst; Diagnosys LLC, Lowell, MA, USA) from an ERG system (Espion, Diagnosys LLC). Eyes that were not exposed were kept shielded with a black photographic cloth during the light exposure procedure in the contralateral eye.

In vivo optical coherence tomography (OCT) imaging and analyses

En face and retinal cross-sectional imaging was performed with the dogs under general inhalation anesthesia as described above. Overlapping *en face* images of

reflectivity with near-infrared illumination (820 nm) were obtained (Spectralis HRA+OCT, Heidelberg, Germany) with 30^{o} and 55^{o} diameter lenses to delineate fundus features such as optic nerve, retinal blood vessels, boundaries of injection blebs, retinotomy sites and other local changes. Custom programs (MatLab 7.5; The MathWorks, Natick, MA) were used to digitally stitch individual photos into a retina-wide panorama. Two methods were used to overlay injection blebs onto panoramic images. In WT eyes, photos of blebs taken at the time of the surgery were registered and bleb boundaries were transferred. In *RHO*-mutant eyes, sketches of blebs drawn at the time of the surgery were transferred onto panoramic images.

Spectral-domain optical coherence tomography (SD-OCT) was performed with linear and raster scans (Spectralis HRA+OCT, Heidelberg, Germany). Overlapping (30^{o}x20^{o}) raster scans were recorded covering large regions of the retina. Post-acquisition processing of OCT data was performed with custom programs (MatLab 7.5; The MathWorks, Natick, MA). For retina-wide topographic analysis, integrated backscatter intensity of each raster scan was used to locate its precise location and orientation relative to retinal features visible on the retina-wide panorama. Individual longitudinal reflectivity profiles (LRPs) forming all registered raster scans were allotted to regularly spaced bins (1^{o}x1^{o}) in a rectangular coordinate system centered at the optic nerve; LRPs in each bin were aligned and averaged. Intensity and slope information of the backscatter signal along each LRP was manually evaluated to segment two boundaries that define the ONL. One boundary was the distal transition of the outer plexiform layer (OPL) peak. The other boundary was the external limiting membrane (ELM) peak. In locations with severe retinal degeneration without a detectable ELM

peak, the second ONL boundary was placed at the most proximal transition to the RPE peak. In addition, the normalized IS/OS backscatter intensity was calculated by subtracting the mean backscatter intensity of the 5 axial samples vitreal to the OPL boundary from the mean backscatter intensity of the 5 axial samples scleral to the ELM boundary; the latter included the IS/OS peak.(44, 74) IS/OS intensities were only mapped in regions of retained inner and outer segment length since compromise of the latter made it impossible to distinguish the IS/OS signal from the RPE/tapetum signal. Topographic results from uninjected control eyes were registered by the center of the ONH and the canine fovea,(83) and maps of control variability were generated defining the 99th percentile confidence intervals. Injected eyes were compared locus-by-locus to the control confidence intervals to generate maps of significant change.

Electroretinography (ERG) recording and analyses

Dogs were pre-medicated with subcutaneous injections of atropine, and acepromazine, and their pupils dilated with atropine (1%), tropicamide (1%) and phenylephrine (10%). After induction with intravenous propofol, dogs were maintained under general inhalation anesthesia (isoflurane), and their pulse rate, oxygen saturation and temperature were monitored for constancy during the entire procedure. Full-field flash electroretinography was performed as previously described(44, 74) on both eyes using a custom-built Ganzfeld dome fitted with the LED stimuli of a ColorDome stimulator (Diagnosys LLC, Lowell, MA). After 20 min of dark adaptation, rod and mixed rod-cone–mediated responses (averaged 4 times) to single 4 ms white flash stimuli of increasing intensities (from -3.74 to 0.51 log cd.s.m^{-2}) were recorded. Following 5

minutes of white light adaptation (1.53 log cd.m^{-2}), cone-mediated signals (averaged 10 times) to a series of single flashes (from -2.74 to 0.51 log cd.s.m^{-2}) and to a 29.4-Hz flicker (averaged 20 times; from -2.74 to 0.26 log cd.s.m^{-2}) stimuli were recorded. Waveforms were processed with a digital low-pass (50 Hz) filter to reduce recording noise if necessary. Amplitudes of the a- and b-waves of the scotopic mixed rod-cone ERG, and the peak to peak amplitudes of the photopic single flash and 29.4 Hz cone flicker were measured.

Retinal histology and immunohistochemistry

Following euthanasia and enucleation, the globes were fixed in 4% paraformaldehyde (PFA) for 3 hrs followed by 2% PFA for 24 hrs, trimmed, cryoprotected in 15-30% sucrose/PBS solution, and embedded in optimal cutting temperature media as previously reported(81). Ten-micrometer-thick serial sections that encompassed the nontreated, the boundary, and the treated/bleb area were cut on a cryostat (Microm HM550; Thermo Fisher Scientific, Kalamazoo, MI). Blood vessel landmarks identified by H&E staining were used to determine the precise location of the retinal cryosections on the vascular pattern of the *en face* cSLO images, as previously reported.(44, 74, 81) Sequential sections were immunolabeled with primary antibodies and cell-specific markers: rod opsin (cat# MAB5316; 1:200 dilution; EMD Millipore, Billerica, MA), goat anti-human cone arrestin (W. Beltran, Univ. of Pennsylvania; 1:100). The antigen–antibody complexes were visualized with fluorochrome-labeled secondary antibodies (Alexa Fluor, 1:200; Molecular Probes, Kalamazoo, MI), and Hoechst 33342 nuclear stain (Molecular Probes) was used to label cell nuclei. H&E-stained sections

were examined by widefield microscopy (Axioplan; Carl Zeiss Meditec, Dublin, CA), and the images were digitally captured (Spot 4.0 camera; Diagnostic Instruments, Sterling Heights, MI) and imported into a graphics program (Illustrator; Adobe, San Jose, CA) for display. Sections labeled for fluorescent immunohistochemistry were examined by confocal microscopy (Leica TCS SP5; Leica Microsystems, Buffalo Grove, IL), and digital images were taken, processed using the Leica Application suite program, and imported into a graphics program (Illustrator; Adobe).

Retinal tissue sampling for RHO RNA and protein quantification

Immediately following enucleation and separation of the posterior cup, 3 mm biopsy punches from treated and untreated neuroretinal areas were individually collected in cryovials, frozen in liquid nitrogen and stored at - 80° C. For *RHO*-mutant dogs retinal sampling was performed under dim red illumination.

RNA extraction and cDNA synthesis

Total RNA was extracted from the punches of neuroretina using Direct-zol RNA Miniprep Kit (Zymo Research, Irvine, CA). cDNA was prepared from total RNA using the High Capacity RNA to cDNA kit (Applied Biosystems, Foster City, CA) following the manufacturer's recommendations.

Absolute quantification of canine and human RHO transcripts in retina

To efficiently determine the ratio between endogenous canine and exogenous human *RHO* transcripts in the same retinal samples specific primer pairs have been

designed for canine (For: 5'-ACAAGACGGGTGTGGTGCGC; Rev: 5'-TCATGGGCGTCGCCTTCACC) and human *RHO* (For: 5'-CCATCAACTTCCTCACGCTCTA; Rev: 5'-TAGGTTGAGCAGGATGTAGTTGAGA). The SYBR green platform was used for the analysis using a primer concentration of 0.15 µM. Real-time PCR was performed in a total volume of 25 µL in 96-well microwell plates on the Applied Biosystems 7500 Real-Time PCR System. All PCRs were performed using cDNA generated from 0.1 ng DNAase-treated RNA. The RT-PCR product was used for construction of an absolute standard curve for individual amplicons representing the canine and human *RHO*. The number of copies of a template was calculated as previously described.(82) The dynamic range of the calibration curves was between 10^3 and 10^7 molecules. Amplification data were analyzed with the 7500 Software version 2.0.1 (Applied Biosystems).

Quantification of Rhodopsin protein

Protein retinal extracts were prepared from 3 mm biopsy punches collected (under dim red illumination for *RHO*-mutant dogs) from treated and untreated neuroretinal areas. After sonication in a buffer containing 0.23M Sucrose, 2 mM EDTA, 5mM TrisHCl, pH 7.4, and protease inhibitors (Halt Protease Inhibitor cocktail, cat. No. 87786, Thermo Fisher Scientific, Waltham, MA.), samples were centrifuged and total protein concentration in the supernatant was measured by the Bradford method. One µg of total protein from each sample was resolved on 8-16% Tris Glycine gel (Invitrogen, Carlsbad, CA), transferred to a nitrocellulose membrane (iBLOT, Invitrogen) and immunoblotted using anti-Rhodopsin antibody (MAB5316, 1:1000 dilution, EMD

Millipore, Billerica, MA) and anti-Histone H3 antibody (ab1791, 1:3000 dilution, Abcam, Cambridge, MA). Protein bands were visualized on a digital imaging system (Odyssey Fc, Licor, Lincoln, NE) after incubation with infrared labeled secondary antibodies (IRDye 680 and IRDye 800, Licor). Amounts of Rhodopsin protein were quantified with the Licor Image Studio v4.0 software using the histone H3 band for normalization.

SUPPLEMENTAL FIGURES

Suppl. Figure S1: Amino acid sequence of human rhodopsin illustrating sites of known mutations and deletions (based on review from Athanasiou et al.(15)) and target sites of shRNAs and ribozyme knock down reagents evaluated in this current study.

Suppl. Figure S2: Digestion of human rhodopsin mRNA by hammerhead ribozyme 525 (*Rz525*). Levels of wild type (white bar) or resistant/hardened (grey bar) *RHO* transcripts measured by luciferase assay in HEK293 cells co-transfected with a plasmid expressing *Rz525*. Results were normalized to the same fusion transcript measured following co-transfection with a plasmid lacking ribozyme (black bar). Error bars represent standard error of the mean. * = $P<0.05$ for resistant/hardened *RHO* relative to wild type *RHO* by Student's t test.

Suppl. Figure S3: Suppression of RHO expression with *Rz525* in WT canine retinas. (**A**) Schematic representation of the retinas of WT dogs injected subretinally with AAV2/5-*Rz525* at 20 or 50 x10^{11} vg/mL titers showing the location of neuroretinal punches used for quantification of canine rhodopsin (RNA and protein) expression. *Dashed lines*, bleb boundaries; blue area: tapetal region. (**B**) Quantification of the levels of endogenous canine RHO RNA remaining in the treated (Tx) retinal area (injected with 50 x10^{11} vg/mL titer) as a percentage of levels measured in the untreated (UnTx) area. (**C**) Representative immunoblot (upper) and quantification of the levels of endogenous canine RHO protein remaining (lower) in the treated retinal area as a percentage of levels measured in the untreated area of eyes injected with 20 or 50 x10^{11} vg/mL titers. OSasOD designation refers to left eye being displayed as right eye for comparability.

Suppl. Figure S4: Suppression of RHO expression with *Rz525* in *RHO*-mutant canine retinas. (**A**) Schematic representation of the retinas of *RHO*-mutant dogs injected with BSS or AAV2/5-*Rz525* at 20 or 100 x10^{11} vg/mL titers showing the location of neuroretinal punches used for quantification of canine rhodopsin (RNA and protein) expression. *Dashed lines*, bleb boundaries; blue area: tapetal region. (**B**) Quantification of the levels of endogenous canine RHO RNA remaining in the treated retinal area as a percentage of levels measured in the untreated area of eyes injected with BSS or AAV2/5-*Rz525* at 20 or 100 x10^{11} vg/mL titers. (**C**) Representative immunoblot (upper) and quantification of the levels of endogenous canine RHO protein remaining (lower) in the treated retinal area as a percentage of levels measured in the untreated area of eyes injected with BSS or AAV2/5-*Rz525* at 20 or 100 x10^{11} vg/mL titers. (**D**) ONL

thickness topography two weeks post light exposure (post LE) in two *RHO*-mutant dog eyes injected 8 weeks earlier with AAV2/5-*Rz525* at 20 or 100 x10^{11} vg/mL titers. *Dotted lines,* bleb boundaries; *dashed lines*, ONL rescue boundaries. (**E**) Multifocal dark lesions (white arrows) visible by NIR cSLO imaging (upper and lower left panels) in both retinas of a *RHO*-mutant dog treated 8 weeks earlier with AAV2/5-*Rz525* at 100 x10^{11} vg/mL correspond on the OCT B scan (upper right panel) to focal nodules of increased reflectivity (white arrows) located in the subretinal space and RPE/choroid, and by histology (lower right panel) to focal inflammatory cell infiltrates. Retinal separation is visible on the OCT B scan (white arrowheads). *Dotted red lines,* bleb boundaries; dashed green line represents location of OCT B scan. OSasOD designation refers to left eye being displayed as right eye for comparability.

Suppl. Figure S5: Inefficient suppression of RHO expression with *shRNA$_{131}$* in WT canine retinas. (**A**) Schematic representation of the fundus of eyes of WT dogs injected with scAAV2/5-*shRNA$_{131}$* at 10 or 50 x10^{11} vg/mL titers showing the location of neuroretinal punches used for quantification of canine rhodopsin (RNA and protein) expression at 8 weeks post-injection. *Dashed lines*, bleb boundaries; blue area: tapetal region. (**B**) Quantification of the levels of endogenous canine RHO RNA remaining in the treated retinal area as a percentage of levels measured in the untreated area of eyes injected with 10 or 50 x10^{11} vg/mL titers. (**C**) Representative immunoblot and quantification of the levels of endogenous canine RHO protein remaining in the treated retinal area as a percentage of levels measured in the untreated area of eyes injected

with 10 or 50 x10^{11} vg/mL titers. OSasOD designation refers to left eye being displayed as right eye for comparability.

Suppl. Figure S6: Individual topographic results of all 10 WT eyes injected with scAAV2/5-*shRNA*$_{820}$ over a range of titers from 1x to 50x10^{11} vg/mL. ONL thickness (left), normalized IS/OS intensity (middle) and loci chosen within (green squares) and outside (red squares) the bleb (right) for quantitation. 2194-OD and similar labels designate the individual animal and eye. All eyes are shown as equivalent right eyes to allow easier comparison. OSasOD designation refers to left eye being displayed as right eye for comparability.

Suppl. Figure S7: Suppression and replacement of rhodopsin with two separate vectors: incomplete protection of rods and retinal toxicity in *RHO*-mutant eyes. (**A-C**) OCT imaging and histological analysis of retinal protection against light exposure (LE) in a *RHO*-mutant eye co-injected with 5x10^{11}vg/mL of scAAV2/5-*shRNA*$_{820}$ and 5x10^{11} vg/mL of scAAV2/5-*RHO*$_{820}$ (Treatment 1:1). (A) ONL thickness topography 7 weeks after injection/before light exposure (post Inj.) and four weeks post light exposure (post LE) *Dotted lines,* bleb boundaries; *red arrow*, location of OCT B scan shown in lower panel. (B) Rhodopsin (Rho, green)/human cone arrestin (hCA, red) co-immunolabeled retinal cryosection showing morphology of the outer nuclear layer (ONL) and outer segments (OS) in treated and untreated (UnTx) areas of the same eye shown in (A). (C) H&E stained retinal microphotograph taken within the treated area showing maximal rescue effect. (**D-F**) Similar analysis as in (A-C) in a *RHO*-mutant eye co-

injected with 5x10^{11}vg/mL of scAAV2/5-*shRNA$_{820}$* and 10 x10^{11} vg/mL of scAAV2/5-*RHO$_{820}$* (Treatment 1:2). (D) ONL thickness topography. *Dotted lines,* bleb boundaries; *dashed lines*, ONL rescue boundaries; *red arrow* corresponds to location of OCT B scan shown in lower panel; white arrows on OCT B scan show increased perivascular thickening and reflectivity. (E) Double fluorescence IHC (Rhodopsin, green; human cone arrestin, red). (F) H&E stained retinal microphotograph taken within the treated area showing limited ONL rescue and severe lesions of perivascular cell infiltration (arrows). (**G**) OCT imaging 11 weeks post injection in a *RHO*-mutant eye co-injected with 5x10^{11}vg/mL of scAAV2/5-*shRNA$_{820}$* and 10 x10^{11} vg/mL of scAAV2/5-*RHO$_{820}$* (Treatment 1:2) but that was not exposed to light. *Dotted lines,* bleb boundaries; *red and white arrows* show locations of single OCT B scans (right panel). OSasOD designation refers to left eye being displayed as right eye for comparability.

Suppl. Figure S8. **Suppression and replacement of rhodopsin with single vector prevents retinal degeneration in *RHO*-mutant retinas (additional data to Fig 4).** **(A-B)** ONL thickness topography after injection/before light exposure (post Inj.) and two weeks post light exposure (post LE) in two *RHO*-mutant dog eyes injected with scAAV2/5-*RHO$_{820}$-shRNA$_{820}$* at 5 x10^{11} vg/mL titer. *Dotted lines,* bleb boundaries; *dashed lines*, ONL rescue boundaries. *Insets*, maps of significance showing retinal regions with ONL thickness (upper) and IS/OS intensity (lower) values compared point by point to the 99th percentile confidence intervals of uninjected controls. (**C-D**) Rhodopsin (Rho, green)/human cone arrestin (hCA, red) co-immunolabeled retinal cryosections showing morphology of the outer nuclear layer (ONL) and outer segments

(OS) in treated and untreated (UnTx) areas of the same eyes shown in (A-B). OSasOD designation refers to left eye being displayed as right eye for comparability.

Suppl. Figure S9. Natural history of disease in *RHO*-mutant ($RHO^{T4R/+}$) dogs housed under different conditions of ambient illumination. (A,B) Pseudocolor ONL topographies of representative dogs housed under cyclic dim-red light (A) or cyclic standard white kennel illumination (B). All eyes are shown as equivalent right eyes. The optic nerve head (black) and major blood vessels (white), tapetum boundary (yellow), and fovea-like region (white ellipse) are overlaid **(C)** *Schematic*, loci selected in five retinal regions for quantitation of ONL thickness. C, central; ST, superotemporal; SN, superonasal; IT, inferotemporal; and IN, inferonasal. Plots of ONL thickness as a function of age at all sampled individual loci shown as a difference from the mean normal value at the same location. Dashed lines delimit 99th percentile of normal variability.

Suppl. Figure S10. Recombinant AAV2/5 vector constructs used in the study. **(A)** Single-stranded AAV carrying a mouse opsin proximal promoter (mOP) driving the expression of a hammerhead ribozyme (*Rz525*) designed to cleave murine, canine and human *RHO* mRNA. (**B**) Self-complementary AAV carrying an H1 RNA polymerase III promoter (H1) driving the expression of a short hairpin RNA ($shRNA_{131}$) designed to cleave canine and human *RHO* mRNA. (**C**) Self complementary AAV carrying an H1 RNA polymerase III promoter (H1) driving the expression of a short hairpin RNA ($shRNA_{820}$) designed to cleave canine and human *RHO* mRNA. (**D**) Self-

complementary AAV carrying a human opsin promoter driving the expression of a replacement human *RHO* mRNA (*RHO*$_{820}$) designed to be resistant to suppression by *shRNA*$_{820}$. (**E**) Self-complementary AAV carrying both the knockdown reagent *shRNA*$_{820}$ and the human resistant replacement *RHO*$_{820}$. TR: AAV2 inverted terminal repeat; mTR: mutant TR; wtTR: wild type TR; SV40 SD/SA: splice donor/acceptor element derived from simian virus 40; hp Rz: hairpin ribozyme; SV40 pA: SV40 derived polyadenylation terminal signal; HSV TK pro: human herpes simplex virus derived thymidine kinase promoter; Neo R: neomycin resistance gene. bGH pA: bovine growth hormone polyadenylation terminal signal; hGFP: humanized GFP.

Suppl. Fig S1

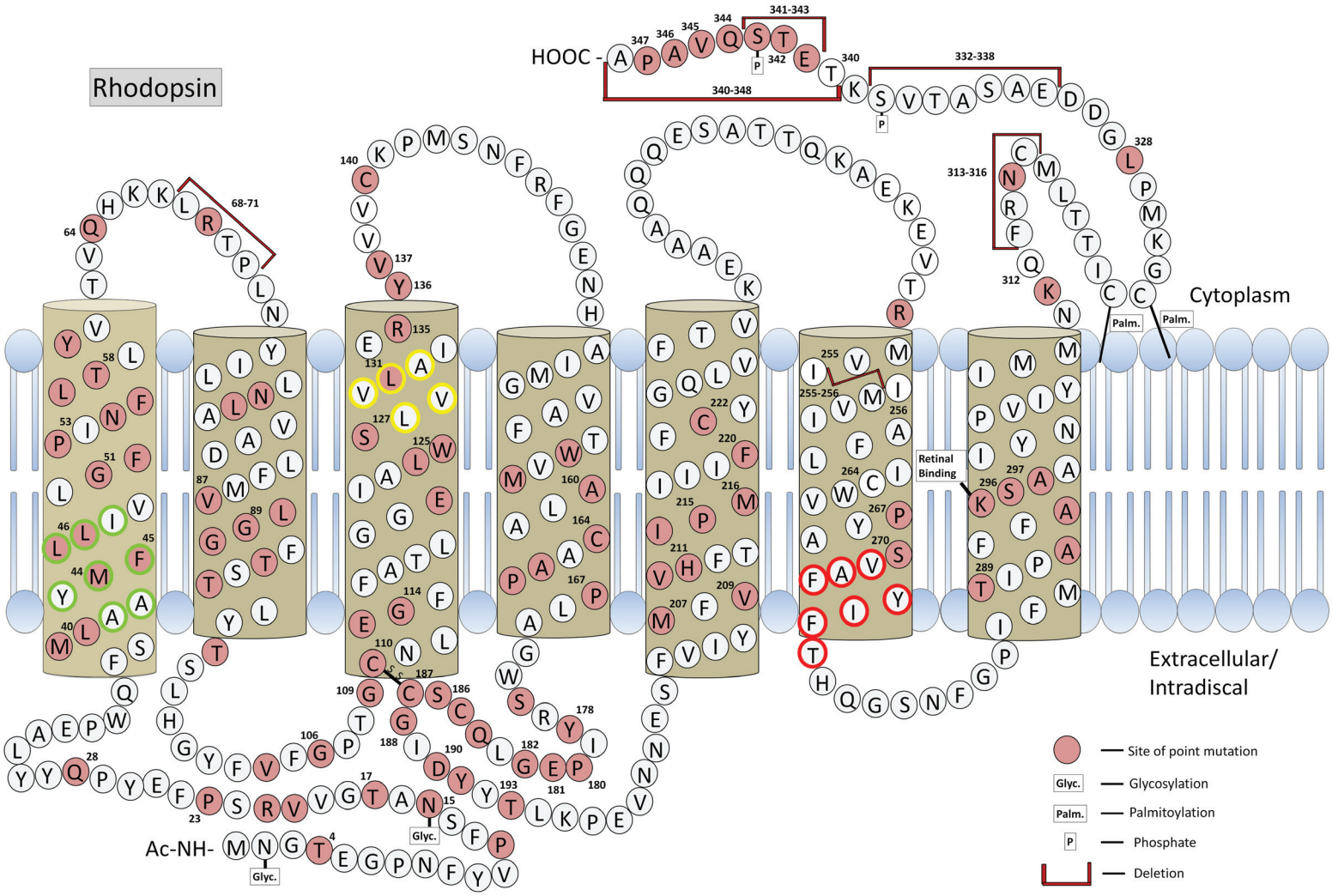

shRNA131 binding site
shRNA134 binding site

Rz525 binding site

RHO820 binding site

Suppl. Fig S2

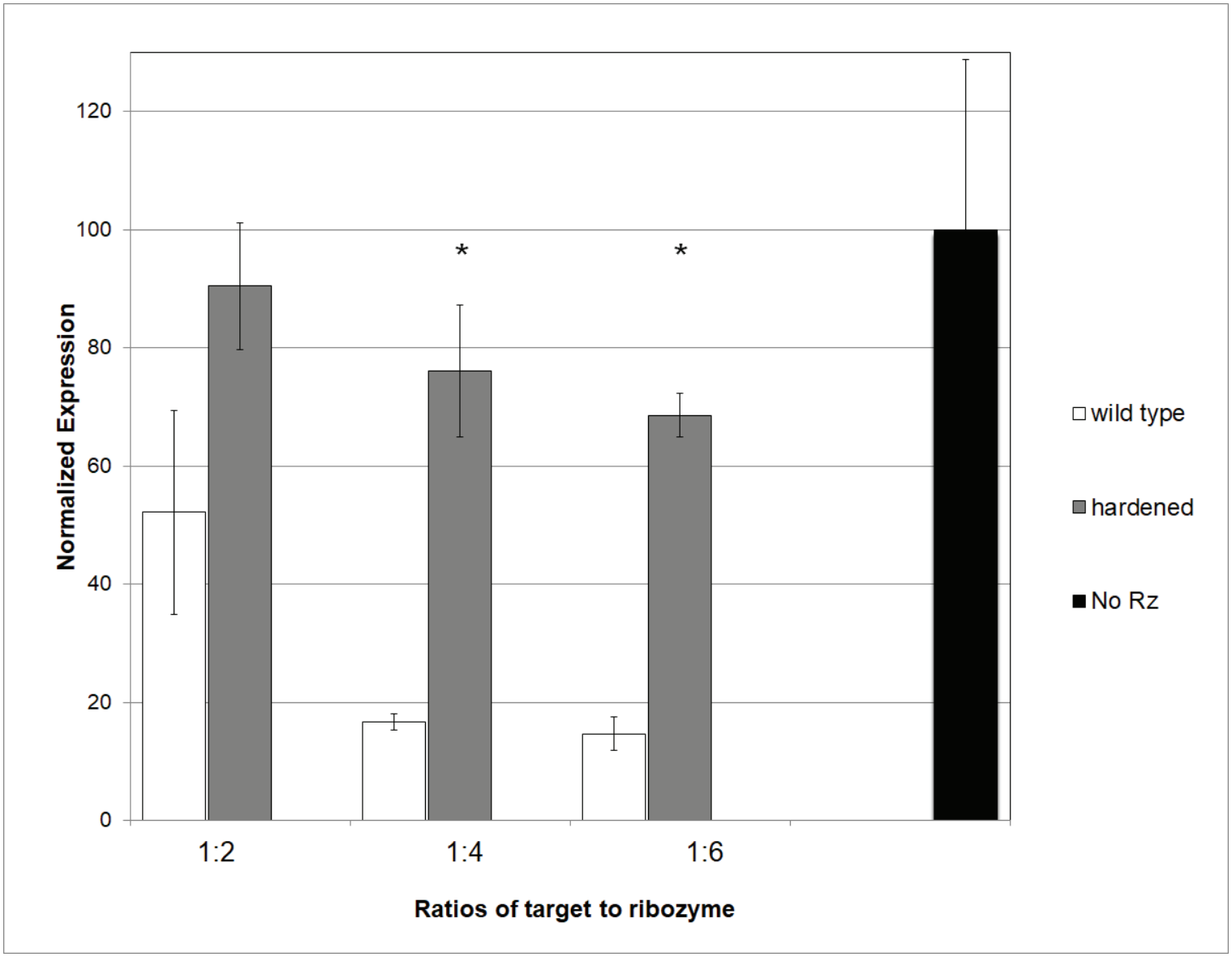
120
100
80
60
40
20
0
Normalized Expression
*
*
1:2
1:4
1:6
Ratios of target to ribozyme
wild type
hardened
No Rz

AAV2/5-mOP-*Rz525* in WT

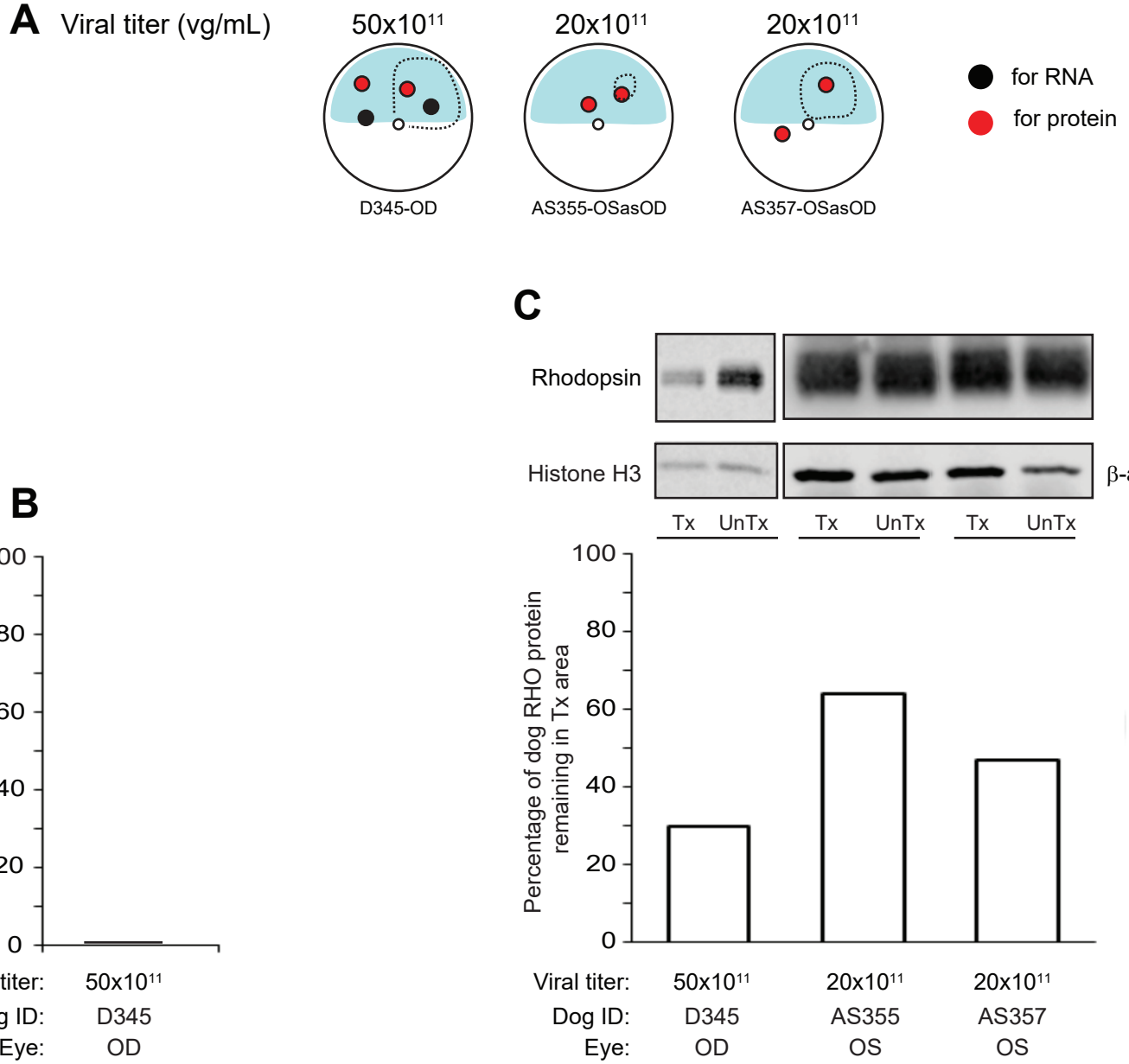

AAV2/5-mOP-*Rz525* in RHO$^{T4R/+}$

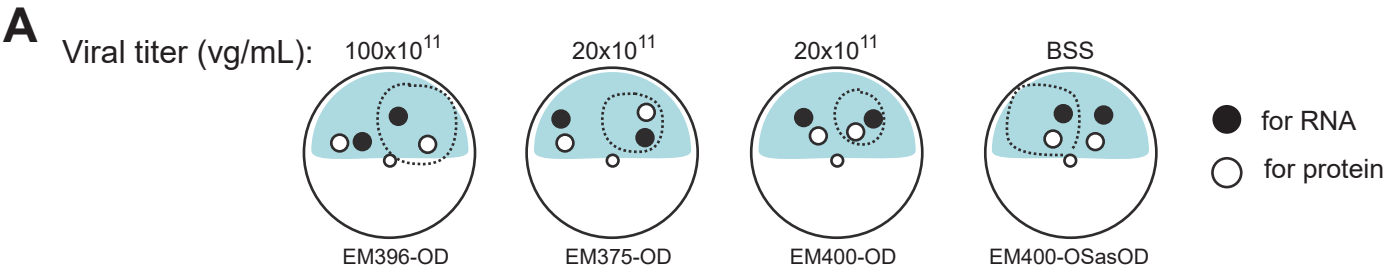

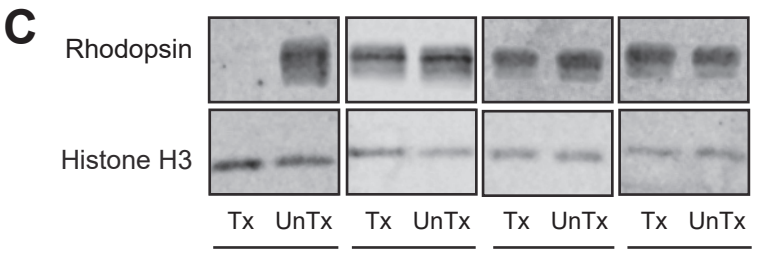

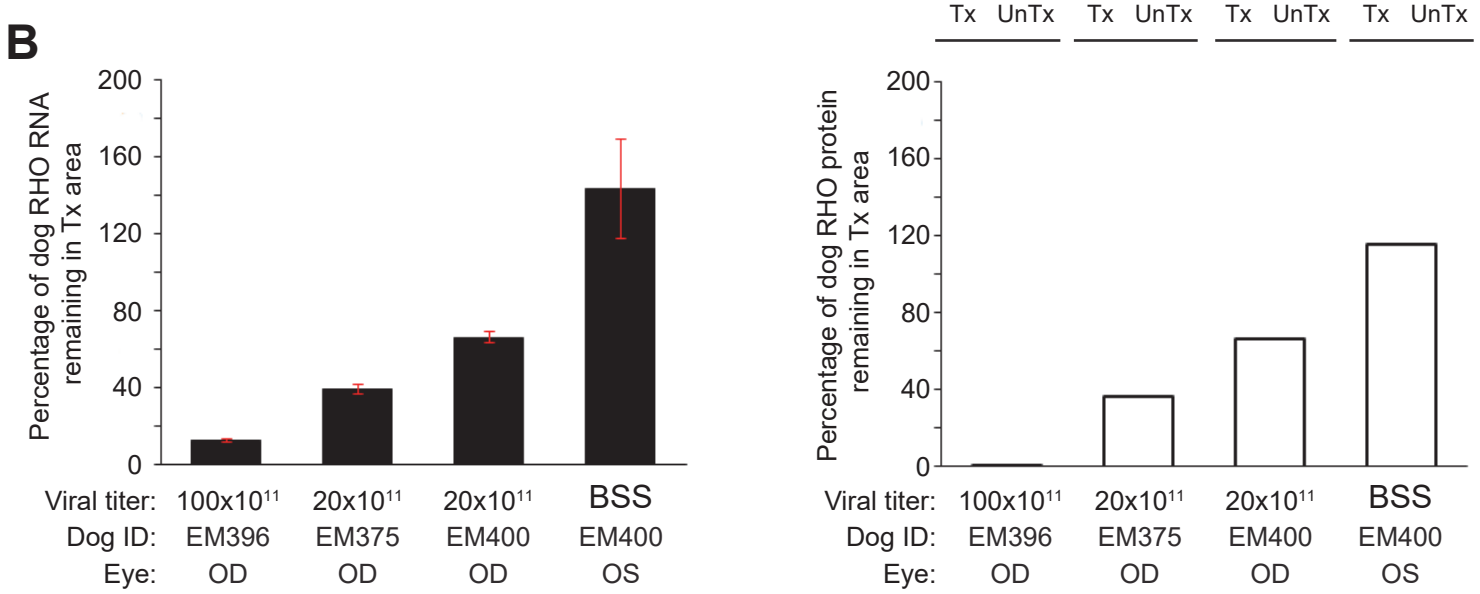

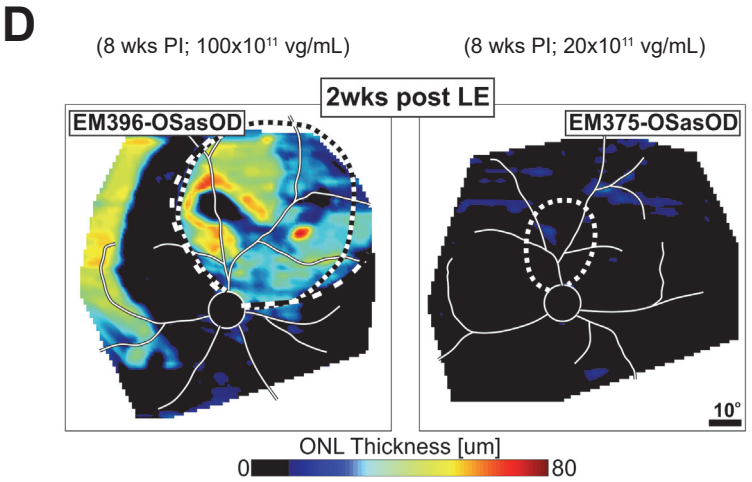

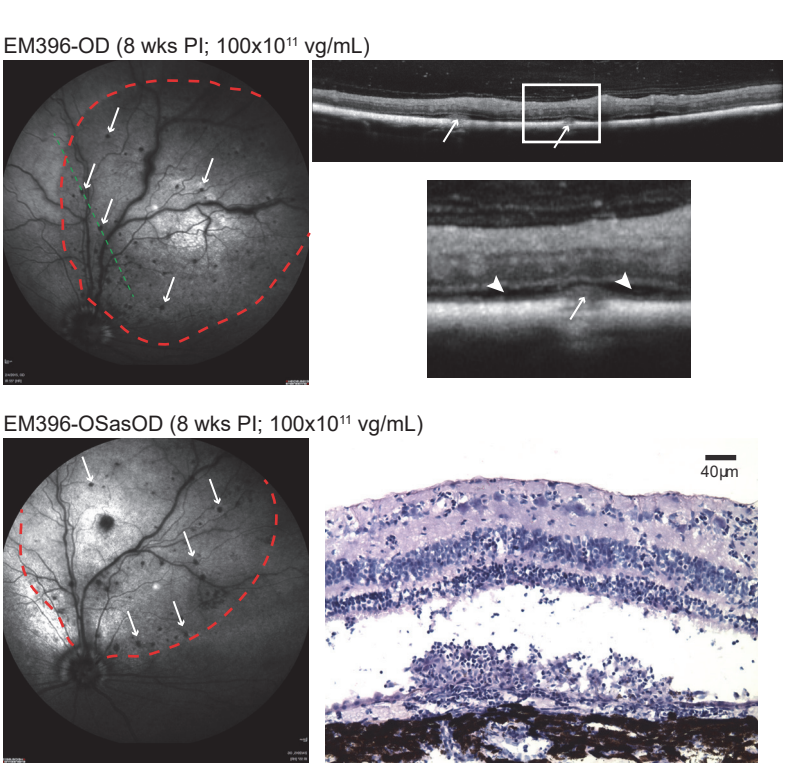

scAAV2/5-H1-*shRNA131* in WT

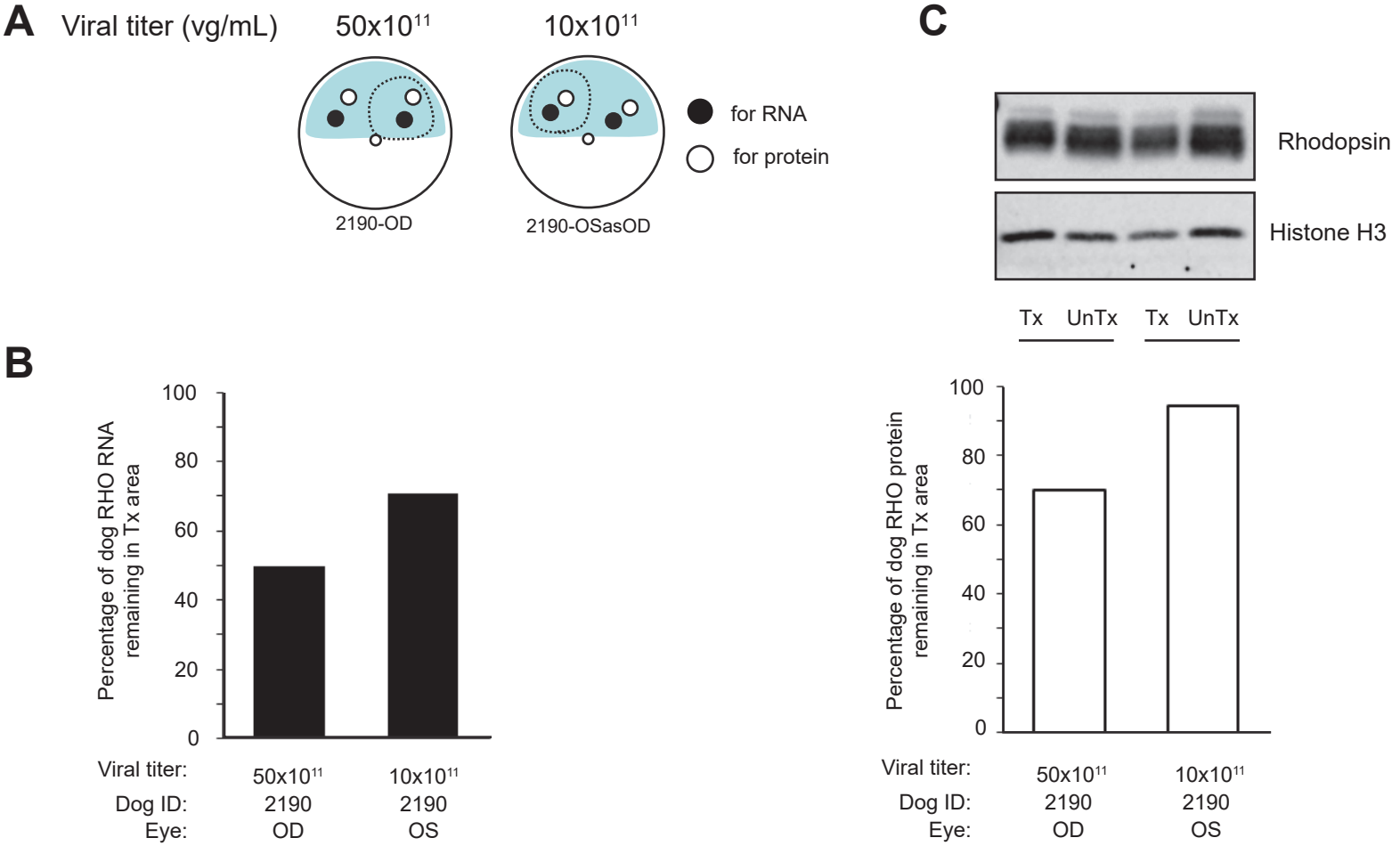

scAAV2/5-H1-*shRNA*820 in WT

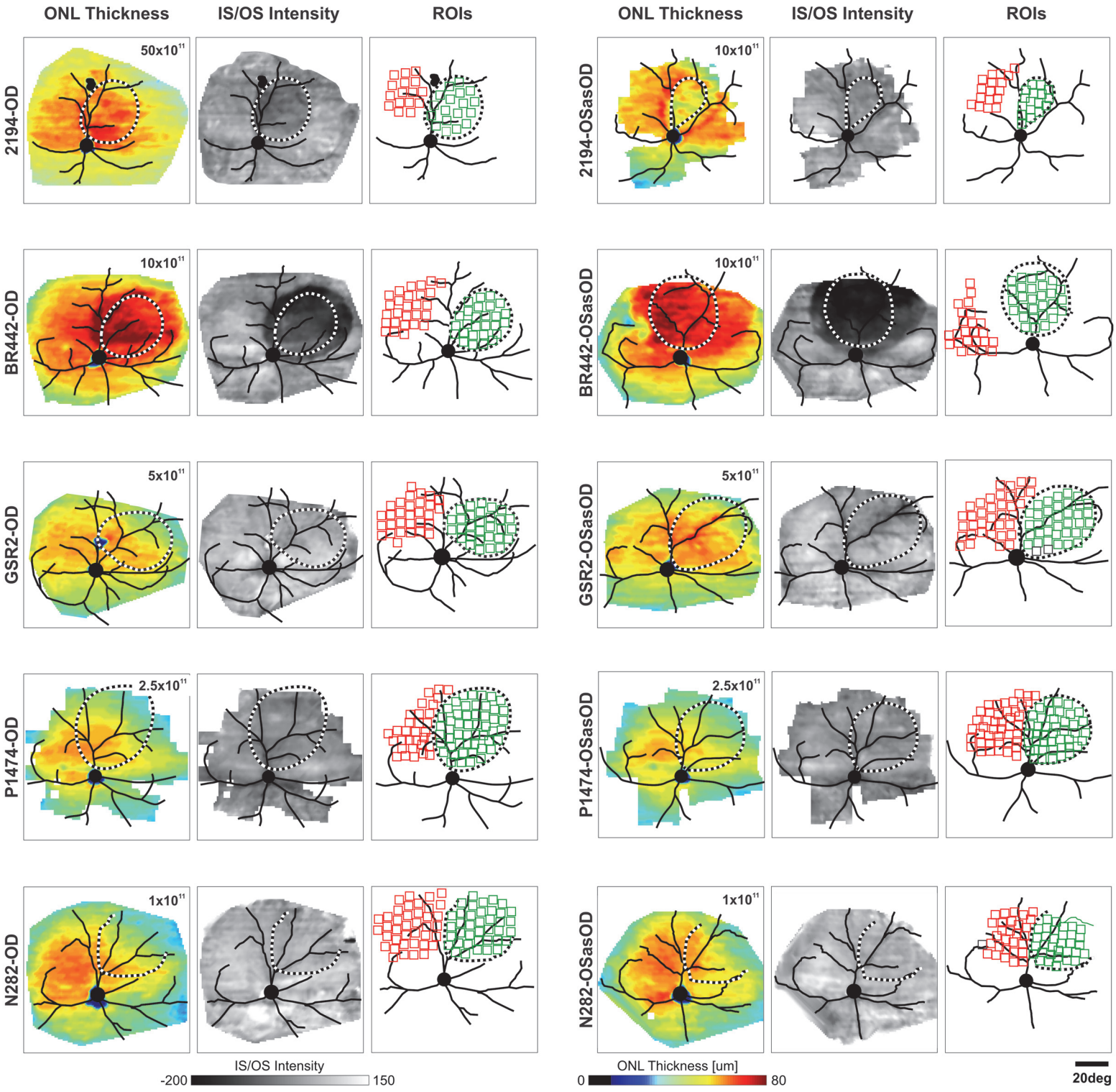

scAAV2/5-H1-sh*RHO820* + scAAV2/5-hOP-*RHO820* in RHO$^{T4R/+}$

Treatment 1:1

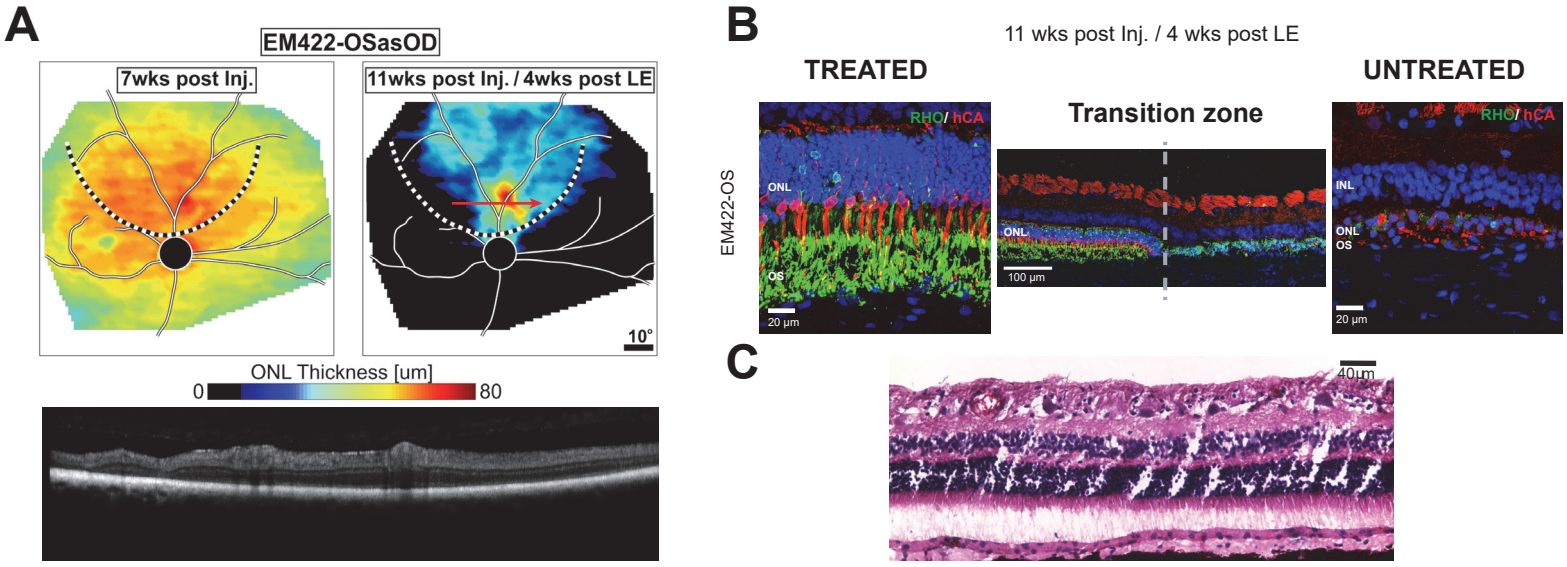

Treatment 1:2

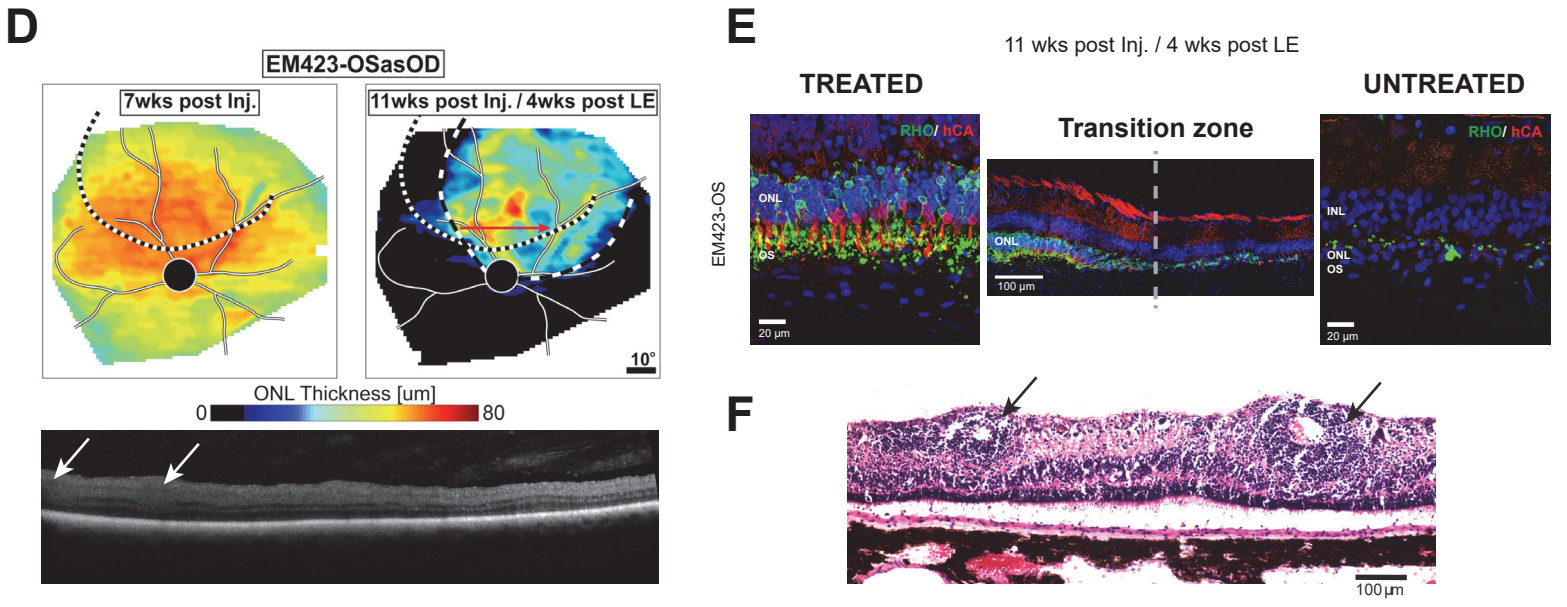

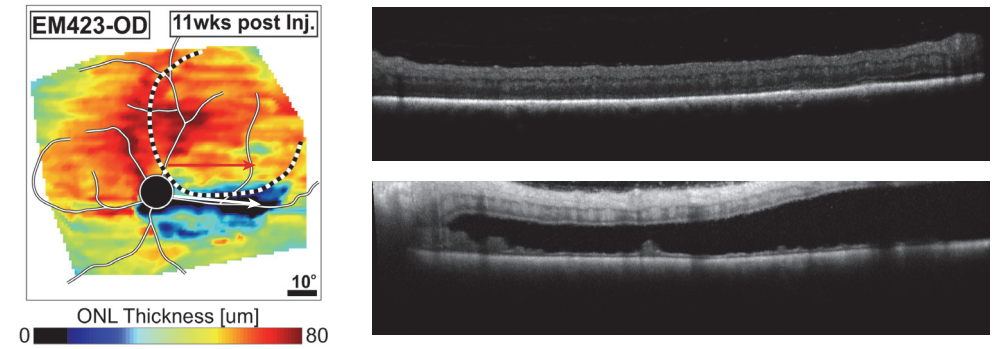

scAAV2/5-hOP-*RHO820*-H1-*shRNA820* in RHO$^{T4R/+}$

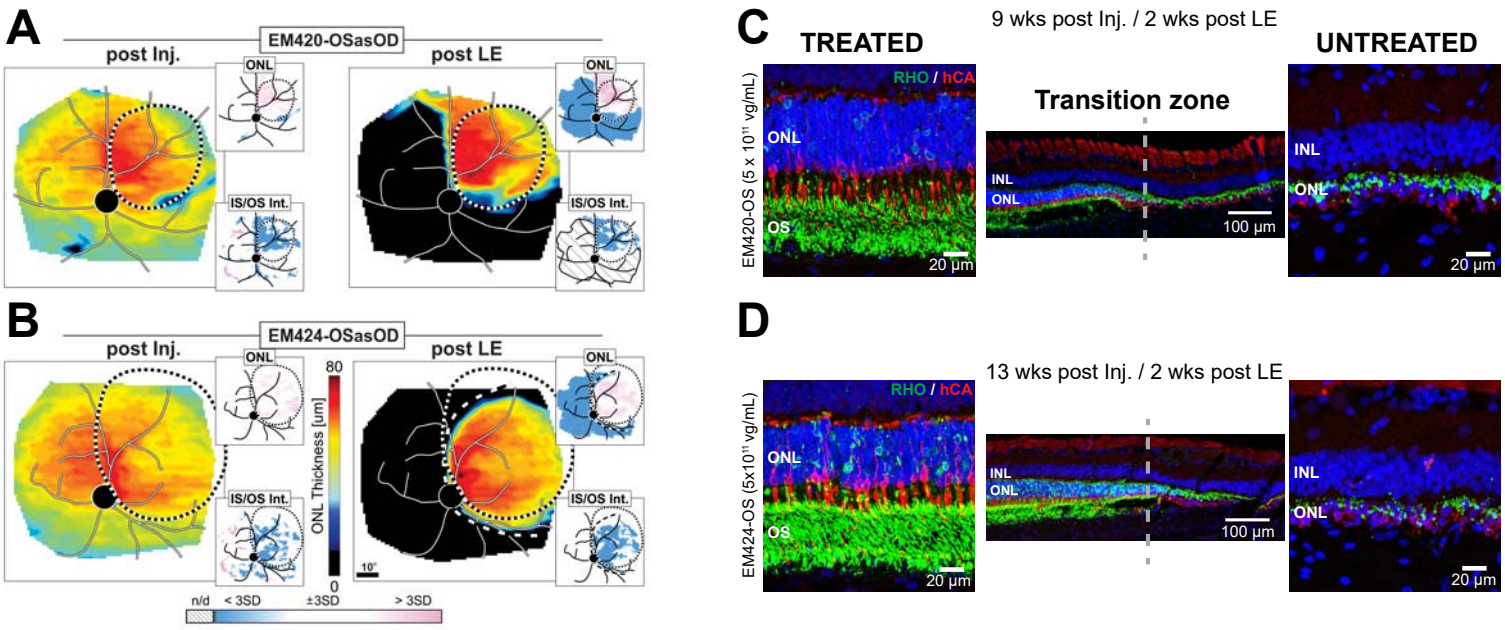

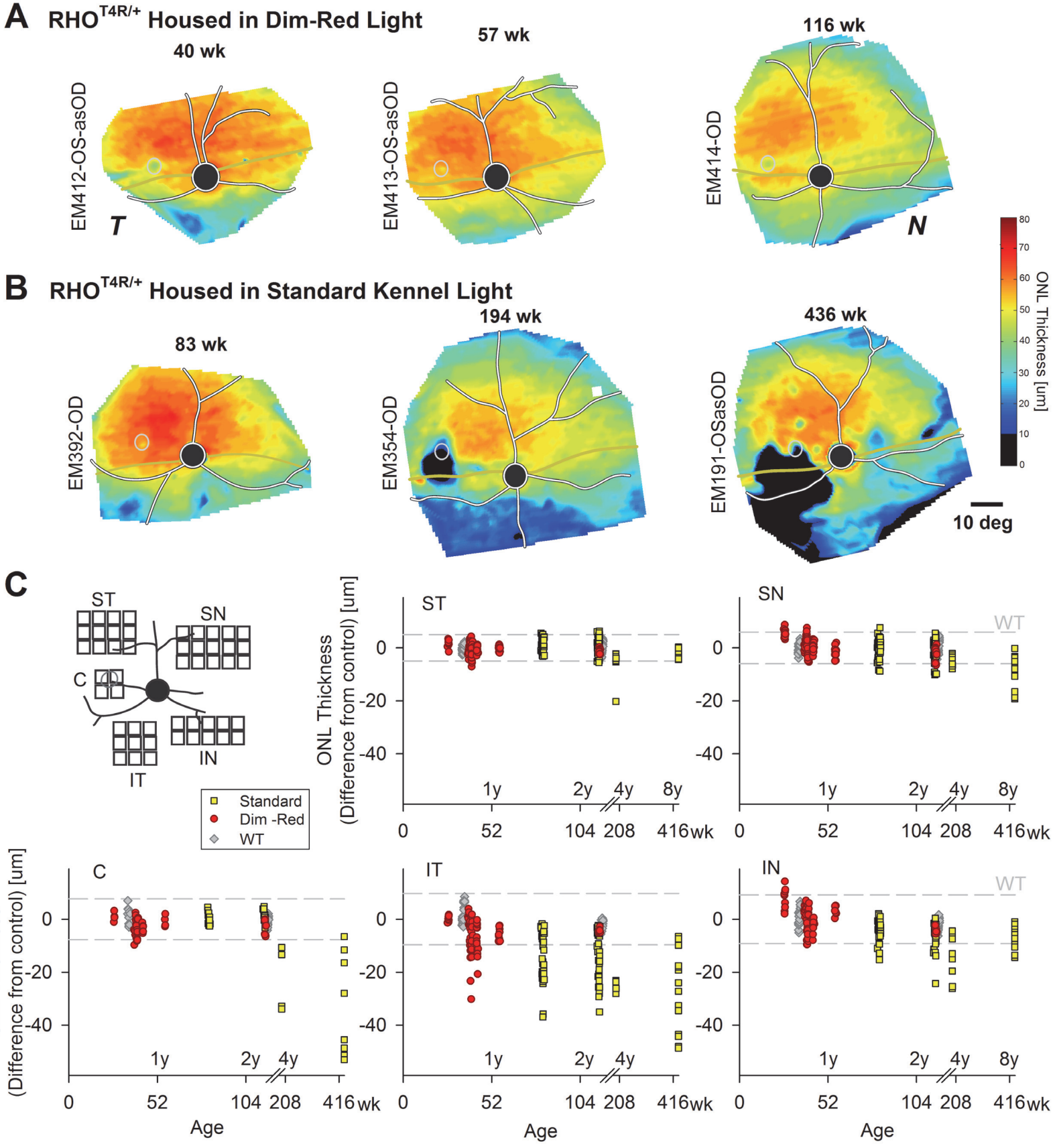
A
RHOT4R/+ Housed in Dim-Red Light
40 wk
57 wk
116 wk
EM412-OS-asOD
EM413-OS-asOD
EM414-OD
T
N
B
RHOT4R/+ Housed in Standard Kennel Light
83 wk
194 wk
436 wk
EM392-OD
EM354-OD
EM191-OSasOD
ONL Thickness [um]
10 deg
C
ST
SN
C
IN
IT
Standard
Dim -Red
WT
ONL Thickness (Difference from control) [um]
1y
2y
4y
8y
0
52
104
208
416wk
Age

A **AAV2/5-mOP-*Rz525***

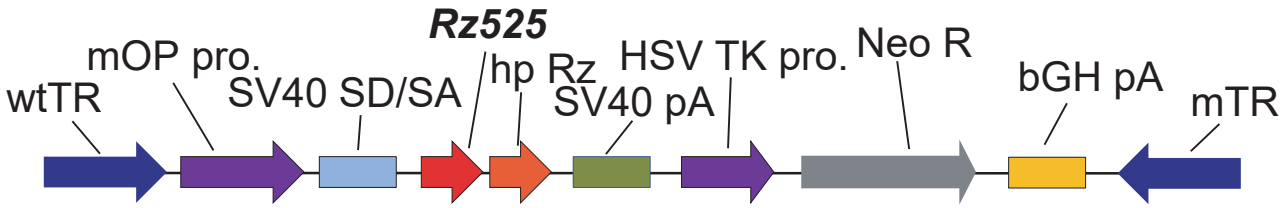

B **scAAV2/5-H1-*shRNA131***

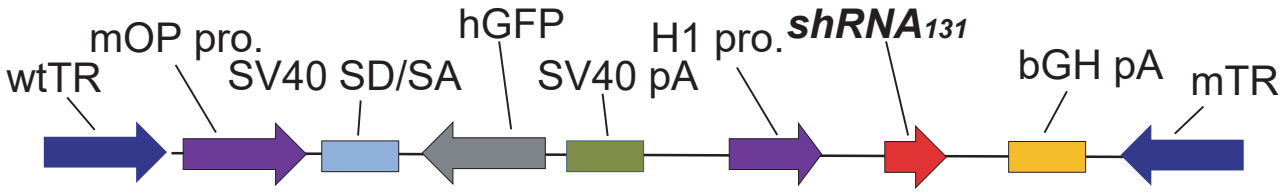

C **scAAV2/5-H1-*shRNA820***

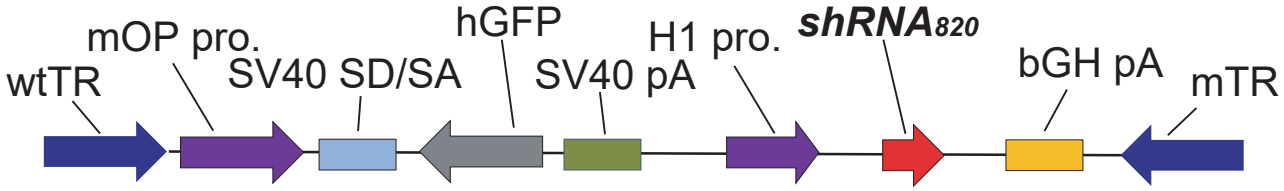

D **scAAV2/5-hOP-*RHO820***

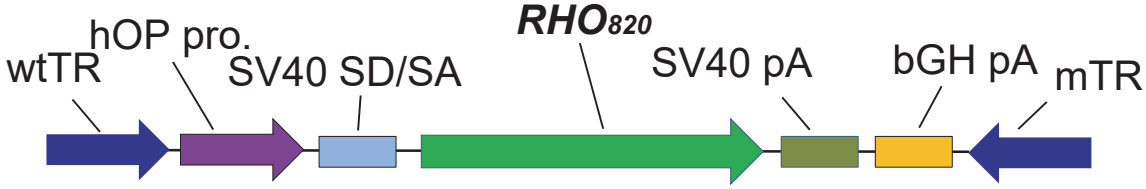

E **scAAV2/5-H1-*shRNA820*-hOP-*RHO820***

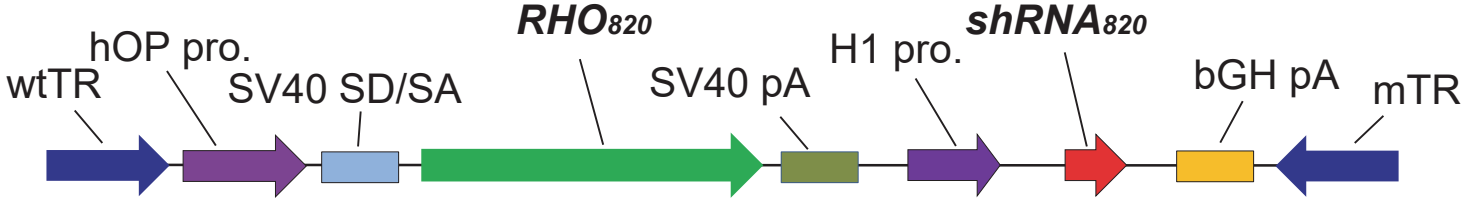

Table S1. Summary of the experimental procedures performed in dogs.

Study/ group	Dog ID-eye	Sex	Treatment	Titer (vg/mL)	Volume (µL)	Dose (vg/eye)	Lights	LE	Analysis	Figure
RHO Knockdown alone in Normal eyes										
A	2194-OD	F	shRNA820	$50x10^{11}$	200 (*50 IVit*)	$100x10^{10}$	white	No	cSLO/OCT; RNA/protein	Fig. 2; S6
	2194-OS	F	shRNA820	$10x10^{11}$	300 (*250 IVit*)	$30x10^{10}$	white	No	cSLO/OCT; RNA/protein	Fig. 2; S6
	BR442-OD	F	shRNA820	$10x10^{11}$	200 (*50 IVit*)	$20x10^{10}$	white	No	cSLO/OCT;H&E/IHC	Fig. 2; S6
	BR442-OS	F	shRNA820	$10x10^{11}$	150	$15x10^{10}$	white	No	cSLO/OCT; RNA/protein	Fig. 2; S6
	GSR2-OD	F	shRNA820	$5x10^{11}$	300 (*150 IVit*)	$15x10^{10}$	white	No	cSLO/OCT;H&E/IHC	Fig. 2; S6
	GSR2-OS	F	shRNA820	$5x10^{11}$	150 (*40 IVit*)	$7.5x10^{10}$	white	No	cSLO/OCT; RNA/protein	Fig. 2; S6
	P1474-OD	M	shRNA820	$2.5x10^{11}$	200 (*50 IVit*)	$5x10^{10}$	white	No	cSLO/OCT; RNA/protein	Fig. 2; S6
	P1474-OS	M	shRNA820	$2.5x10^{11}$	150	$3.7x10^{10}$	white	No	cSLO/OCT;H&E/IHC	Fig. 2; S6
	N282-OD	M	shRNA820	$1x10^{11}$	150	$1.5x10^{10}$	white	No	cSLO/OCT;H&E/IHC	Fig. 2; S6
	N282-OS	M	shRNA820	$1x10^{11}$	160	$1.6x10^{10}$	white	No	cSLO/OCT; RNA/protein	Fig. 2; S6
							white			
B	2190-OD	M	shRNA131	$50x10^{11}$	150	$75x10^{10}$	white	No	RNA/protein	Fig. S5
	2190-OS	M	shRNA131	$10x10^{11}$	150	$15x10^{10}$	white	No	RNA/protein	Fig. S5
							white			
C	D345-OD	F	Rz525	$50x10^{11}$	150	$75x10^{10}$	white	No	RNA/protein	Fig. S3
	AS355-OS	F	Rz525	$20x10^{11}$	150	$30x10^{10}$	white	No	RNA/protein	Fig. S3
	AS357-OS	F	Rz525	$20x10^{11}$	150	$30x10^{10}$	white	No	RNA/protein	Fig. S3
RHO Knockdown alone in RHO$^{T4R/+}$ mutant eyes										
D	EM408-OD	F	shRNA820	$10x10^{11}$	200 (*50 IVit*)	$20x10^{10}$	red	No	cSLO/OCT	
	EM409-OD	F	shRNA820	$10x10^{11}$	150	$15x10^{10}$	red	No	cSLO/OCT; RNA/protein	Fig. 3
	EM411-OD	F	shRNA820	$5x10^{11}$	160	$8x10^{10}$	red	No	cSLO/OCT; RNA/protein	Fig. 3
	EM413-OD	F	shRNA820	$2.5x10^{11}$	150	$3.7x10^{10}$	red	No	cSLO/OCT; RNA/protein	Fig. 3
	EM412-OD	F	shRNA820	$1x10^{11}$	220 (*70 IVit*)	$2.2x10^{10}$	red	No	cSLO/OCT; RNA/protein	Fig. 3
E	EM408-OS	F	shRNA820	$10x10^{11}$	150	$15x10^{10}$	red	Yes	cSLO/OCT	Fig. S9
	EM409-OS	F	shRNA820	$10x10^{11}$	150	$15x10^{10}$	red	Yes	cSLO/OCT;H&E/IHC	Fig. 3, S9
	EM411-OS	F	shRNA820	$5x10^{11}$	150	$7.5x10^{10}$	red	Yes	cSLO/OCT;H&E/IHC	Fig. 3, S9
	EM413-OS	F	shRNA820	$2.5x10^{11}$	150	$3.7x10^{10}$	red	Yes	cSLO/OCT;H&E/IHC	Fig. 3, S9
	EM412-OS	F	shRNA820	$1x10^{11}$	150	$1.5x10^{10}$	red	Yes	cSLO/OCT;H&E/IHC	Fig. 3, S9
F	EM396-OD	M	Rz525	$100x10^{11}$	150	$150x10^{10}$	white	No	cSLO/OCT; RNA/protein	Fig. S4
	EM375-OD	M	Rz525	$20x10^{11}$	300 (*150 IVit*)	$60x10^{10}$	white	No	cSLO/OCT; RNA/protein	Fig. S4
	EM400-OD	F	Rz525	$20x10^{11}$	150 (*40 subRPE*)	$30x10^{10}$	white	No	RNA/protein	Fig. S4
	EM400-OS	F	BSS	/	150	/	white	No	RNA/protein	Fig. S4
	EM396-OS	M	Rz525	$100x10^{11}$	150	$150x10^{10}$	white	Yes	cSLO/OCT; H&E	Fig. S4
	EM375-OS	M	Rz525	$20x10^{11}$	450 (300 *IVit*)	$90x10^{10}$	white	Yes	cSLO/OCT	

RHO Knockdown and Replacement: two vector strategy in RHO$^{T4R/+}$ mutant eyes										
G	EM422-OD	M	(shRNA820) + (RHO820)	$5x10^{11}$ + $5x10^{11}$	150	$15x10^{10}$	red	No	cSLO/OCT	
	EM423-OD	M	(shRNA820) + (RHO820)	$5x10^{11}$ + $10x10^{11}$	150	$22.5x10^{10}$	red	No	cSLO/OCT	Fig. S7
	EM422-OS	M	(shRNA820) + (RHO820)	$5x10^{11}$ + $5x10^{11}$	150	$15x10^{10}$	red	Yes	cSLO/OCT; H&E/IHC	Fig. S7, S9
	EM423-OS	M	(shRNA820) + (RHO820)	$5x10^{11}$ + $10x10^{11}$	150	$22.5x10^{10}$	red	Yes	cSLO/OCT; H&E/IHC	Fig. S7
RHO Knockdown and Replacement: single vector strategy in RHO$^{T4R/+}$ mutant eyes										
H	EM418-OD	M	(shRNA820 + RHO820)	$5x10^{11}$	150	$7.5x10^{10}$	red	No	RNA/protein	Fig. 4
	EM420-OD	F	(shRNA820 + RHO820)	$5x10^{11}$	150	$7.5x10^{10}$	red	No	RNA/protein	Fig. 4
	EM424-OD	M	(shRNA820 + RHO820)	$5x10^{11}$	150	$7.5x10^{10}$	red	No	RNA/protein	Fig. 4
	EM425-OD	M	(shRNA820 + RHO820)	$5x10^{11}$	150	$7.5x10^{10}$	red	No	RNA/protein	Fig. 4
	EM418-OS	M	(shRNA820 + RHO820)	$5x10^{11}$	150	$7.5x10^{10}$	red	Yes	cSLO/OCT; IHC	Fig. 4, S9
	EM420-OS	F	(shRNA820 + RHO820)	$5x10^{11}$	150	$7.5x10^{10}$	red	Yes	cSLO/OCT; IHC	Fig. S8, S9
	EM424-OS	M	(shRNA820 + RHO820)	$5x10^{11}$	150	$7.5x10^{10}$	red	Yes	cSLO/OCT; IHC	Fig. S8, S9
	EM425-OS	M	(shRNA820 + RHO820)	$5x10^{11}$	150	$7.5x10^{10}$	red	Yes	cSLO/OCT; IHC	Fig. 4
RHO Knockdown and Replacement: single vector strategy in RHO$^{T4R/+}$ mutant eyes (Long-term follow-up after multiple LD exposures)										
I	EM426-OD	M	(shRNA820 + RHO820)	$5x10^{11}$	150	$7.5x10^{10}$	red	Yes	cSLO/OCT; ERG	Fig. 5
	EM428-OD	F	(shRNA820 + RHO820)	$5x10^{11}$	150	$7.5x10^{10}$	red	Yes	cSLO/OCT; ERG	Fig. 5
	EM426-OS	M	BSS	/	150	/	red	Yes	ERG	Fig. 5
	EM428-OS	F	BSS	/	150	/	red	Yes	ERG	Fig. 5
Natural history in RHO$^{T4R/+}$ mutant eyes (uninjected eyes or pre-injection time points)										
J	EM414-OD	M	None	/	/	/	red	No	cSLO/OCT	Fig. S9
	EM392-OD	M	None	/	/	/	white	No	cSLO/OCT	Fig. S9
	EM392-OS	M	None	/	/	/	white	No	cSLO/OCT	Fig. S9
	EM393-OD	F	None	/	/	/	white	No	cSLO/OCT	Fig. S9
	EM393-OS	F	None	/	/	/	white	No	cSLO/OCT	Fig. S9
	EM354-OD	F	None	/	/	/	white	No	cSLO/OCT	Fig. S9
	EM191-OD	M	None	/	/	/	white	No	cSLO/OCT	Fig. S9
	EM191-OS	M	None	/	/	/	white	No	cSLO/OCT	Fig. S9
WT Control eyes										
K	CGBCAN-OD	M	None	/	/	/	white	No	cSLO/OCT	Fig. S9
	CGBCDI-OD	M	None	/	/	/	white	No	cSLO/OCT	Fig. S9
	CGBCGS-OD	M	None	/	/	/	white	No	cSLO/OCT	Fig. S9
	N292-OS	M	None	/	/	/	white	No	cSLO/OCT	Fig. S9
	N293-OS	F	None	/	/	/	white	No	cSLO/OCT	Fig. S9
	N294-OS	F	None	/	/	/	white	No	cSLO/OCT	Fig. S9

Lights: cyclic environmental (12 hrs ON, 12 hrs OFF) dim red or white illumination; LE: light exposure protocol; OD: right eye; OS: left eye; F: female; M: male; IVit: intravitreal; subRPE: under the retinal pigment epithelium; cSLO: confocal scanning laser ophthalmoscopy; OCT: optical coherence tomography; RNA/Protein: Quantification of rhodopsin RNA and protein levels; ERG: electroretinography; H&E: histology with hematoxylin & eosin staining; IHC: immunohistochemistry.

Table S2: Codon frequency (per thousand) at target site of WT *RHO* and at codon-modified resistant site of *hRHO$_{820}$* (based on Codon Usage Database, http://www.kazusa.or.jp/codon/).

Species	**WT *RHO***	**Resistant *hRHO$_{820}$***
	GCA	GCU
Dog	13.7	17.2
Human	15.8	18.4
	UUC	UUU
Dog	24.4	17.1
Human	20.3	17.6
	UAC	UAU
Dog	17.5	11.5
Human	15.3	12.2
	AUC	AUA
Dog	25.7	7.2
Human	20.8	7.5
	GCA+UUC+UAC+AUC	GCU+UUU+UAU+AUA
Dog	81.3	53
Human	72.2	55.7